Optimization design and manufacturing tolerance analysis of a polymer microring resonant wavelength multiplexer

Chun-Sheng Ma
Jilin University
College of Electronic Science and Engineering
State Key Laboratory of Integrated Optoelectronics
Changchun 130023, China
and
Chinese Academy of Sciences
Changchun Institute of Optics, Fine Mechanics, and Physics
State Key Laboratory of Applied Optics
Changchun 130021, China

Xian-Yin Wang
Jilin University
College of Electronic Science and Engineering
State Key Laboratory of Integrated Optoelectronics
Changchun 130023, China
E-mail: wxyrcl@yahoo.com.cn

Shu-Lin E
Chinese Academy of Sciences
Changchun Institute of Optics, Fine Mechanics, and Physics
State Key Laboratory of Applied Optics
Changchun 130021, China

Yuan-Zhe Xu
Xin Yan
Da-Ming Zhang
Jilin University
College of Electronic Science and Engineering
State Key Laboratory of Integrated Optoelectronics
Changchun 130023, China

Zhan-Chen Cui
Jilin University
College of Chemistry
Changchun 130023, China

De-Gui Sun
Chinese Academy of Sciences
Changchun Institute of Optics, Fine Mechanics, and Physics
State Key Laboratory of Applied Optics
Changchun 130021, China

Abstract. Based on formulas presented, optimization design is performed and the effects of manufacturing tolerances on transmission characteristics are analyzed for a polymer microring resonant wavelength multiplexer around the central wavelength of 1.550918 μm with wavelength spacing 1.6 nm. Modeling results show that the insertion loss is less than 0.55 dB and crosstalk is less than -21 dB for each of eight vertical output channels of the designed device without tolerances. Some manufacturing tolerances result in a shift of the transmission spectrum and lead to increases of the inserted loss and crosstalk over the design case without tolerances. [DOI: 10.1117/1.1842777]

Subject terms: microring resonance; wavelength multiplexer; manufacturing tolerance; transmission spectrum; insertion loss; crosstalk.

Paper 040161 received Mar. 25, 2004; revised manuscript received Aug. 11, 2004; accepted for publication Aug. 11, 2004; published online Feb. 1, 2005.

1 Introduction

As the basic elements of optoelectronic devices, microring resonators have many promising applications, such as filters,[1,2] modulators,[3] lasers, and others,[4–6] due to their simpler structures, easier fabrication, and greater compactness.[7] The wavelength multiplexer composed of microring resonators is a novel kind of device in wavelength division multiplexing (WDM) optical systems.[8–10] This kind of microring resonant wavelength multiplexer (MRRWM), fabricated from polymer materials,[3] possess

0091-3286/2005/$22.00 © 2005 SPIE

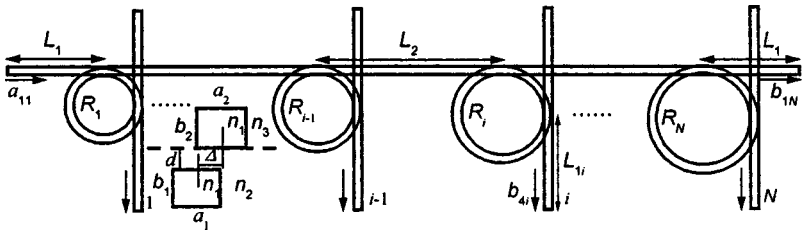

Fig. 1 Schematic diagram of a MRRWM, where the insert shows the cross sections and refractive index profiles of the channel and microring, and where $\lambda=1.550918\ \mu$m, $n_1=1.6278$, $n_2=1.465$, $n_3=1$.

some excellent features, including lower insertion loss, smaller crosstalk, easier integration, better thermal stability and temperature dependence, smaller birefringence, and easier control of the refractive index.

Excellent MRRWMs are dependent on accurate structural design and fine technology. However, manufacturing tolerances are hard to avoid in the fabrication of the devices. Therefore, parameter optimization and manufacturing tolerance analysis are very important in the design and fabrication of MRRWMs.

This paper is organized as follows. First, in Sec. 2, we report in detail the parameter optimization of a 1×8 polymer MRRWM around the central wavelength of 1.550918 μm with a wavelength spacing of 1.6 nm. The optimized parameters include the core thickness and core width of the channels and microrings, microring radii, radius difference of adjacent microrings, resonant order, free spectral range (FSR), and number of vertical output channels. Then, in Sec. 3, effects of manufacturing tolerances on the transmission spectrum, inserted loss, and crosstalk are investigated. Finally, conclusions are summarized in Sec. 4.

2 Optimization Design

A schematic diagram of the MRRWM investigated in this paper is shown in Fig. 1, in which a horizontal main input channel is crossed over N vertical output channels. In every filter element,[11] a microring is placed on the top of the main channel and the corresponding vertical channel; between them a coupling layer exists. The insert shows the cross sections and refractive index profiles of the channel and microring. Let a_1 and b_1 be the width and thickness of the channels, and a_2 and b_2 be those of the microrings. Assume that the channel and microring have the same core refractive index n_1, but have different cladding refractive indices n_2 and n_3, respectively, and assume that n_2 also is the refractive index of the coupling layer.

Let the total length of the main channel be $2L_1+(N-1)L_2$, where L_1 is the distance from the input or output port of the main channel to the adjacent coupling point, and L_2 is that between adjacent coupling points on the main channel, and let $L_{1i}=L_1-(i-1)\Delta R$ be the distance from the output port of the ith vertical channel to the adjacent coupling point. Assume that L_2 is sufficiently large so that the coupling between the vertical output channel and the next microring can be neglected. Denote by a_{11}, b_{1N} the signal amplitudes at the input and output ports of the main channel, respectively, and by b_{4i} that at the output port of the ith vertical channel.

Let N signals with different wavelengths $\lambda_i=\lambda_1+(i-1)\Delta\lambda$ resonate in N respective microrings with different radii $R_i=R_1+(i-1)\Delta R$, where $i=1,2,...,N$, and where $\Delta\lambda$ and ΔR are the wavelength spacing and radius difference of adjacent microrings, respectively. Let m_i be the resonant order, and n_c be the mode effective refractive index. From the microring resonant equation $2\pi R_i n_c=m_i\lambda_i$, we can derive the expressions for the microring radius R_i, radius difference ΔR_i, the corresponding free spectral range FSR_i, and the maximum number $N_{\max}$ of vertical output channels in FSR_i as, respectively,

$$R_i=\frac{m_i\lambda_i}{2\pi n_c}, \tag{1}$$

$$\Delta R_i=\frac{1}{2\pi n_c}\left(\lambda_i\Delta m+\frac{m_i n_g}{n_c}\Delta\lambda\right), \tag{2}$$

$$\mathrm{FSR}_i=\frac{\lambda_i n_c}{m_i n_g}, \tag{3}$$

$$N_{\max}=\mathrm{int}\left(\frac{\mathrm{FSR}_i}{\Delta\lambda}\right), \tag{4}$$

where $n_g=n_c-\lambda\,\mathrm{d}n_c/\mathrm{d}\lambda$ is the group refractive index, and $\Delta m=m_{i+1}-m_i$ is the resonant order difference of the adjacent microrings. In the following calculations, we take the central resonant wavelength to be $\lambda_5=1.550918\ \mu$m, the refractive index of the polymer cores of the channels and microrings to be $n_1=1.6278$, that of the claddings of the channels to be $n_2=1.465$ [that is, the relative refractive index difference is $\Delta n=(n_1-n_2)/n_1=0.1$], and that of the claddings of the microrings to be $n_3=1.0$. The values of the parameters used in the calculation are given in the corresponding figure captions.

By solving the mode eigenvalue equation of the rectangular optical waveguide,[12] the curves of the mode effective refractive index n_c versus the core thicknesses b_1 and b_2 are plotted in Fig. 2. We find that when we choose $a_1=b_1=1.48\ \mu$m, $a_2=2.01\ \mu$m, and $b_2=1.576\ \mu$m, only the fundamental modes can propagate in the device. Furthermore, E_{00}^{x} (dashed curves) and E_{00}^{y} (solid curves) of channels have the same mode propagation constant β as those of $\mathrm{E}_{00}^{\prime x}$ (dashed curves) and $\mathrm{E}_{00}^{\prime y}$ (solid curves) of microrings. This means that the mode birefringence is already elimi-

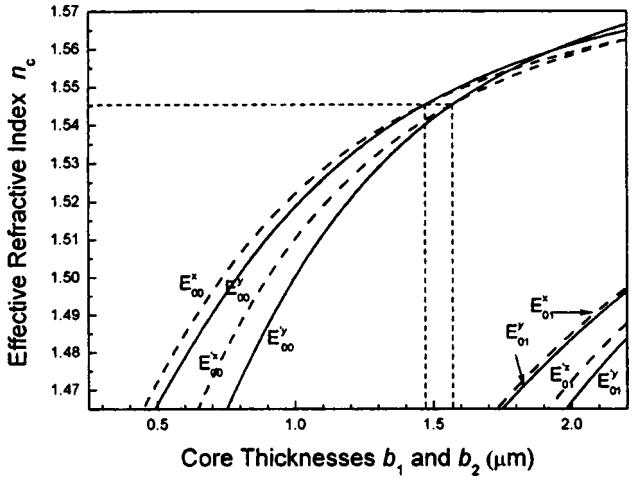

Fig. 2 Curves of n_c versus b_1 and b_2, where $a_1=1.48\,\mu$m, $a_2=2.01\,\mu$m, E_{pq}^x (dashed curves) and E_{pq}^y (solid curves) correspond to the channels, and $E_{pq}^{'x}$ (dashed curves) and $E_{pq}^{'y}$ (solid curves) correspond to the microrings.

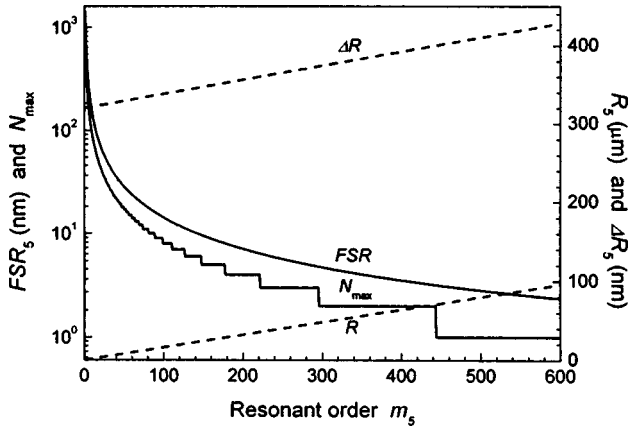

Fig. 4 Curves of R_5, ΔR_5, FSR_5, and $N_{\max}$ versus m_5, where $a_1=b_1=1.48\,\mu$m, $a_2=2.01\,\mu$m, $b_2=1.576\,\mu$m.

nated, and the polarization independence of the device is realized. Therefore, in the following analysis we assume that all the channels and microrings possess the same mode propagation constant β.

Figure 3 shows the curves of the mode effective refractive index n_c versus the operating wavelength λ. It can be seen that the operating wavelength λ should be limited within the range of 1.54 to 1.56 μm to maintain the single-mode propagation. Furthermore, the eight resonant wavelengths λ_1 to λ_8 are covered in this wavelength range, and the mode birefringence is very small, and hence the polarization dependence is very weak.

Figure 4 shows the dependence on the resonant order m_5 of the microring radius R_5, the radius difference ΔR_5, FSR_5, and the maximum number $N_{\max}$ for the central wavelength λ_5. We find that as m_5 increases, R_5 and ΔR_5 increase, while FSR_5 and $N_{\max}$ decrease. It is known from Fig. 4 that m_5 and Δm need to be selected properly. If m_5 is too small, R_5 will be too small, which will bring about large bending loss. On the contrary, if m_5 is too large, FSR_5 and $N_{\max}$ will be too small, making it difficult to realize the demultiplexing of the device. On the other hand, if Δm is taken to be zero, then ΔR_5 has to be about 16.45 nm for $m_5=105$, and it is very difficult to realize such a small distance between adjacent microrings in the fabrication of the device. Considering the conditions of our laboratory and the practical structure of the device, we select $\Delta m=2$, and $m_5=105$ for the central wavelength λ_5. In this case, ΔR_5 can be increased to 338.21 nm, which will be of benefit in the fabrication of the device. At the same time, the FSR is about 13.58 nm, so eight resonant wavelengths can be inserted in a FSR around the central wavelength λ_5, whereas in the design presented in Refs. 8 and 9, the eight resonant wavelengths were inserted in three consecutive FSRs, which would lead to measurement inconvenience in demultiplexing.

Figure 5 plots the curves of the bending loss coefficient $2\alpha_b$ versus the microring radius R for the fundamental modes $E_{00}^{'x}$ and $E_{00}^{'y}$, which is calculated from the formula presented in Ref. 13. It is found that the bending loss co-

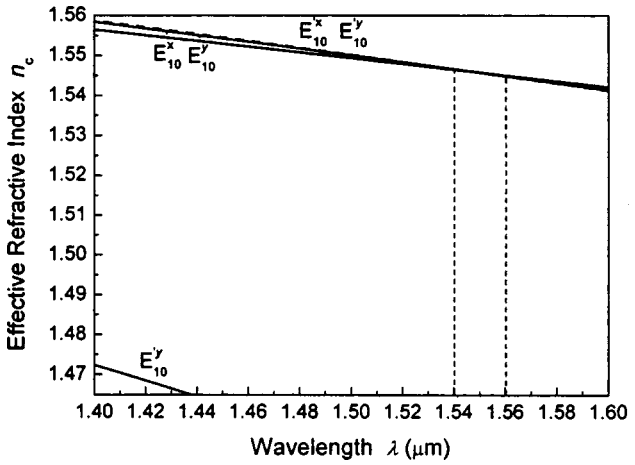

Fig. 3 Curves of n_c versus λ, where $a_1=b_1=1.48\,\mu$m, $a_2=2.01\,\mu$m, $b_2=1.576\,\mu$m.

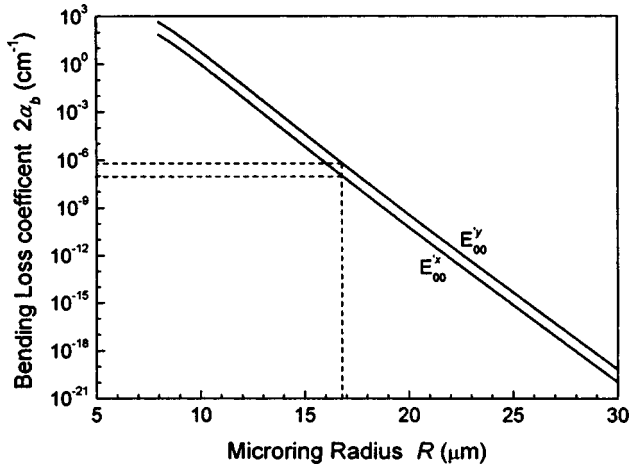

Fig. 5 Curves of $2\alpha_b$ versus R for the $E_{00}^{'x}$ and $E_{00}^{'y}$ fundamental modes, where $a_2=2.01\,\mu$m, $b_2=1.576\,\mu$m.

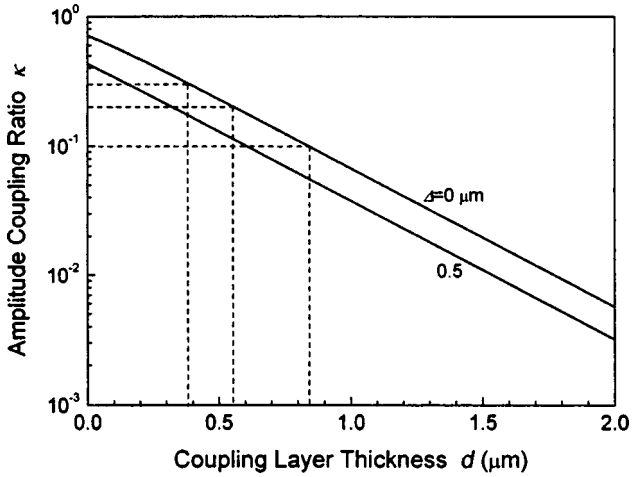

Fig. 6 Curves of κ_i versus d for, where $a_1=b_1=1.48\,\mu$m, $a_2=2.01\,\mu$m, $b_2=1.576\,\mu$m, $R=16.77\,\mu$m, and the deviation $\Delta=0$, 0.5 μm.

efficient $2\alpha_b$ decreases as the microring radius R increases. When we take R to be 16.77 μm, $2\alpha_b$ drops to about 1.1×10^{-7}/cm and 6.2×10^{-7}/cm for the $E_{00}'^{x}$ and $E_{00}'^{y}$ fundamental modes, respectively, which is much smaller than the propagation loss coefficient $2\alpha_p=0.1$/cm.

By means of controlling the variation of the thickness d of the coupling layer and the deviation Δ between the channel and the microring, we can enable the amplitude coupling ratios of all the filter elements to have the same value κ.

Figure 6 shows the relation between the amplitude coupling ratio κ and the coupling layer thickness d between channels and microrings, which is calculated from the mode coupling theory.[14] It can be seen that the amplitude coupling ratio κ can be limited to the range 0.3 to 0.1 when the coupling layer thickness d is varied from 0.38 to 0.84 μm for the coupling deviation $\Delta=0$. When we take κ to be 0.2, the coupling layer thickness d is about 0.55 μm.

In summary, the optimized values of the parameters of the polymer MRRWM are listed in Table 1.

3 Manufacturing Tolerance Analysis

In terms of the mode coupling theory[14] and the transfer matrix technique,[15,16] we can derive the transfer function from the input port to the output port of the main channel $|B_N|^2$ and that from the input port of the main channel to the output port of the ith vertical channel $|D_i|^2$ as, respectively,

$$|B_N|^2=\left|\frac{b_{1N}}{a_{11}}\right|^2=\left|\left(\prod_{i=1}^{N}U_i\right)\exp[-j(N-1)\psi_2]\times\exp(-j2\psi_1)\right|^2, \tag{5}$$

$$|D_i|^2=\left|\frac{b_{4i}}{a_{11}}\right|^2=\left|\left(\prod_{k=1}^{i-1}U_k\right)V_i\exp[-j(i-1)\psi_2]\times\exp[-j(\psi_{1i}+\psi_1)]\right|^2, \tag{6}$$

with

$$U_i=\frac{t\{1-\exp[-j(\phi_{1i}+\phi_{2i})]\}}{1-t^2\exp[-j(\phi_{1i}+\phi_{2i})]},$$

$$V_i=-\frac{\kappa^2\exp(-j\phi_{2i})}{1-t^2\exp[-j(\phi_{1i}+\phi_{2i})]}, \tag{7}$$

Table 1 Optimized values of parameters of a polymer MRRWM for the fundamental mode.

Central wavelength	$\lambda_5=1.550918\,\mu$m
Wavelength spacing	$\Delta\lambda=1.6$ nm
Refractive index of polymer cores of channels and microrings	$n_1=1.6278$
Refractive index of polymer claddings of channels	$n_2=1.465$
Refractive index of air claddings of microrings	$n_3=1.0$
Relative refractive index difference	$\Delta n=(n_1-n_2)/n_1=0.1$
Core width and thickness of channels	$a_1=b_1=1.48\,\mu$m
Core width of microrings	$a_2=2.01\,\mu$m
Core thickness of microrings	$b_2=1.576\,\mu$m
Resonant order for central microring	$m_5=105$
Resonant order difference of adjacent microrings	$\Delta m=2$
Central microring radius	$R_5=16.768\,\mu$m
Radius difference of adjacent microrings	$\Delta R=0.338\,\mu$m
Free spectral range	$FSR_5=13.58$ nm
Number of vertical output channels	$N_{max}=8$
Distance	$L_1=4000\,\mu$m
Distance	$L_2=250\,\mu$m

$$\psi_1 = L_1(\beta - j\alpha_L), \quad \psi_{1i} = L_{1i}(\beta - j\alpha_L),$$

$$\psi_2 = L_2(\beta - j\alpha_L), \tag{8a}$$

$$\phi_{1i} = 3\pi R_i(\beta - j\alpha_{Ri})/2, \quad \phi_{2i} = \pi R_i(\beta - j\alpha_{Ri})/2, \tag{8b}$$

where $t=(1-\kappa^2)^{1/2}$, $\alpha_L=\alpha_p$, and $\alpha_{Ri}=\alpha_{bi}+\alpha_p$ are the propagation loss coefficients of the channels and the ith microring, respectively, which includes the bending loss α_{bi} and the propagation loss α_p. The insertion loss and crosstalk of every vertical channel are defined as, respectively,

$$L^{(i)}\ (\mathrm{dB}) = -10\log_{10}(|D_i|^2), \tag{9}$$

$$L_{\mathrm{CT}}^{(i)}(\lambda_i)\ (\mathrm{dB}) = 10\log_{10}\left[\sum_{j\neq i,j=1}^{N} |D_j(\lambda_i)|^2 \Big/ |D_i(\lambda_i)|^2\right], \tag{10}$$

where $i=1,2,...,N$.

In the following calculation, we take account of the propagation loss of channels and microrings whose coefficient $2\alpha_p$ is about 0.1/cm, and the bending loss of microrings whose coefficient $2\alpha_{Ri}$ is about 1.1×10^{-7}/cm for the central microring radius $R_5=16.768\,\mu$m.

Using the formulas given, first the transmission spectra of the eight vertical output channels are plotted in Fig. 7(a), and that around the central resonant wavelength λ_5 is plotted in Fig. 7(b). It can be seen from Fig. 7(a) that the eight resonant wavelengths with wavelength spacing 1.6 nm in a FSR can be output from the eight corresponding vertical channels, and wavelength demultiplexing is realized in the device. The minimum output intensity of the nonresonant light is about 3.9×10^{-4}. It can also be seen from Fig. 7(b) that the resonant peak of the transmission spectrum possesses a Lorentzian shape, and its 3-dB bandwidth is about 0.18 nm when we take κ to be 0.2. Because of the plausible optimization of the relative parameters, the curves of the transmission spectra of the fundamental modes $E_{pq}^{'x}$ are coincident with those of the fundamental modes $E_{pq}^{'y}$.

In the fabrication of the device, it is difficult to control the exact design values of some parameters, such as κ, Δn, and R, so the corresponding manufacturing tolerances δ_κ, $\delta_{\Delta n}$, and δ_R must be accepted, and hence affect the transmission characteristics of the device.

Figure 8 shows the effects of the tolerances δ_κ, $\delta_{\Delta n}$, and δ_R on the transmission spectra of the eight vertical output channels. We find that only $\delta_{\Delta n}$ or δ_R shifts the spectrum; δ_κ does not. Figure 8(a) shows that when δ_κ varies from negative to positive, the 3-dB bandwidth of the resonant peak increases, and the minimum output nonresonant intensity becomes large. When we take δ_κ to be 0, that is, $\kappa=0.2$, the 3-dB bandwidth is about 0.18 nm; this is the design case without tolerances. Figures 8(b) and 8(c) show that the resonant peaks shift to the left when $\delta_{\Delta n}$ or δ_R is negative, but to the right when $\delta_{\Delta n}$ or δ_R is positive. When we take $|\delta_{\Delta n}|=0.0002$ or $|\delta_R|=3.5$ nm, the shift of the transmission spectrum is about 0.35 nm with respect to the designed case without tolerances.

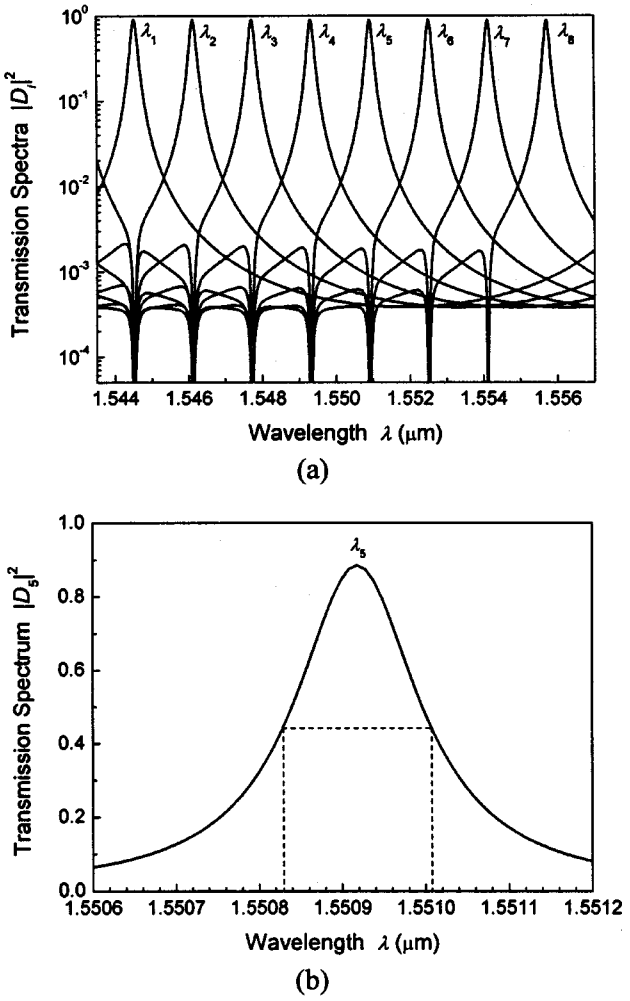

Fig. 7 (a) Transmission spectra of eight vertical output channels, and (b) that around the central resonant wavelength λ_5, where $2\alpha_p=0.1$/mm, and the values of the other parameters are listed in Table 1.

Figure 9 shows the effects of the tolerances δ_κ, $\delta_{\Delta n}$, and δ_R on the insertion loss of the eight vertical output channels. We find that δ_κ, $\delta_{\Delta n}$, and δ_R result in an increase of the insertion loss, whether they are negative or positive.

Figure 10 shows the effects of the tolerances δ_κ, $\delta_{\Delta n}$, and δ_R on the crosstalk of the eight vertical output channels. It can be seen from Fig. 10(a) that when δ_κ is negative, that is, κ decreases, the crosstalk decreases. On the contrary, if δ_κ is positive, that is, κ increases, the crosstalk increases. It can also be seen from Figs. 10(b) and 10(c) that the effects of $\delta_{\Delta n}$ and δ_R on the crosstalk are minor compared with the design case without tolerances, except for the first vertical output channel.

4 Conclusions

On the basis of the preceding optimization design and manufacturing tolerance analysis of a 1×8 polymer MRRWM around the central wavelength of 1.550918 μm with wavelength spacing 0.8 nm, we may conclude as follows.

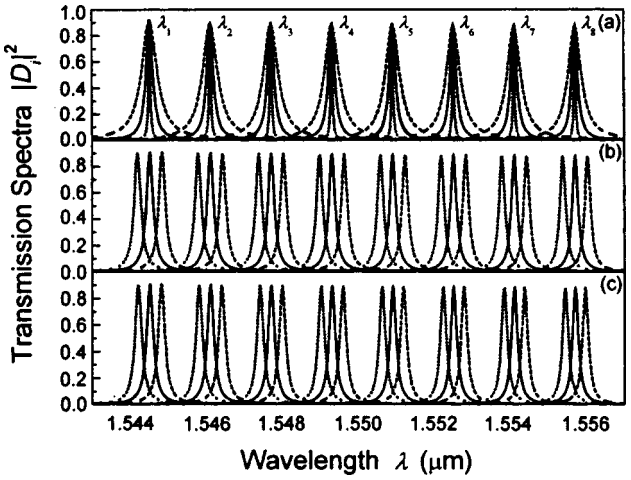

Fig. 8 Effects of (a) δ_κ, (b) $\delta_{\Delta n}$, and (c) δ_R on the transmission spectra of the eight vertical output channels, where $2\alpha_p = 0.1$/mm, and the values of other parameters are listed in Table 1: (a) $\delta_\kappa = -0.1$ (dotted line), 0 (solid line), 0.1 (dashed line); (b) $\delta_{\Delta n} = -0.0002$ (dotted line), 0 (solid line), 0.0002 (dashed line); (c) $\delta_R = -3.5$ (dotted line), 0 (solid line), 3.5 nm (dashed line).

Selecting the central resonant order to be 105, we can produce a central microring radius of 16.768 μm and a FSR of 13.58 nm. We enable the microrings in different filter elements to resonate at different resonant orders to increase the ring radius difference; for example, choosing a resonant order difference of 2 can lead to a radius difference of adjacent microrings of 0.338 μm, which would be of benefit in the fabrication of the device. For every vertical output channel of the designed device without tolerances, when the amplitude coupling ratio is equal to 0.2, the insertion loss is less than 0.55 dB and the crosstalk is less than -21 dB. The manufacturing tolerance of either the microring radii or the relative refractive index difference causes a shift of the transmission spectrum, and results in an increase of the insertion loss and crosstalk. Therefore, we must control the manufacturing tolerances within a proper range to maintain the normal demultiplexing of the device. Currently this kind of polymer MRRWM is being fabricated in our laboratory.

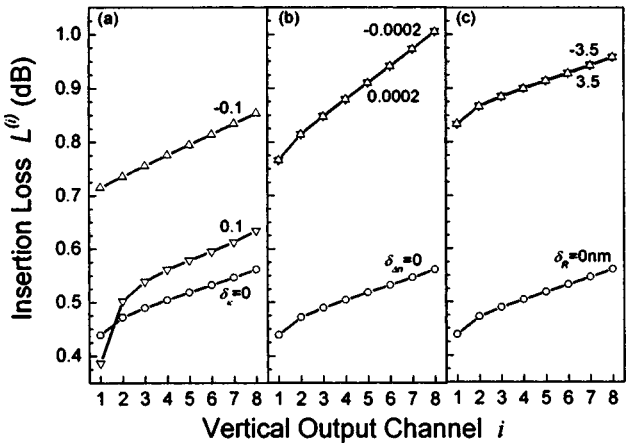

Fig. 9 Effects of (a) δ_κ, (b) $\delta_{\Delta n}$, and (c) δ_R on the insertion loss of the eight vertical output channels, where the values of the parameters are the same as those of Fig. 8.

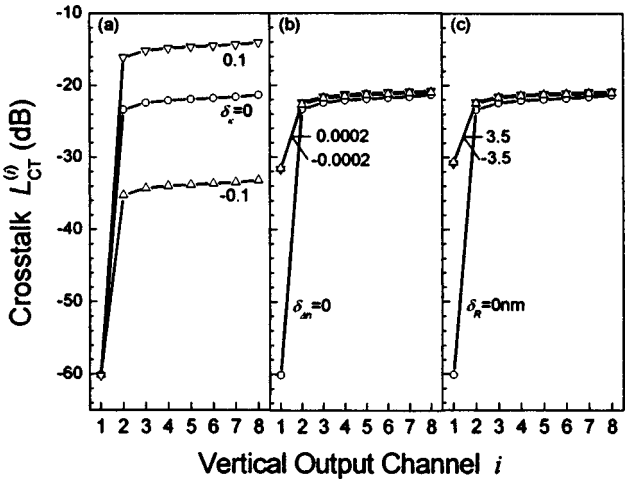

Fig. 10 Effects of (a) δ_κ, (b) $\delta_{\Delta n}$, and (c) δ_R on the crosstalk of the eight vertical output channels, where the values of the parameters are the same as those of Fig. 8.

Acknowledgment

This work was supported by the National Science Foundation Council of China and the Chinese Academy of Sciences (One Hundred Talent Project).

References

1. B. E. Little, S. T. Chu, H. A. Haus, J. Foresi, and J. P. Laine, "Microring resonator channel dropping filters," *J. Lightwave Technol.* **15**(6), 998–1005 (1997).
2. M. K. Chin and S. T. Ho, "Design and modeling of waveguide-coupled single-mode microring resonator," *IEEE J. Lightwave Technol.* **16**(8), 1433–1445 (1998).
3. P. Rabiei, W. H. Steier, C. Zhang, and L. R. Dalton, "Polymer microring filters and modulators," *J. Lightwave Technol.* **20**(5), 1968–1975 (2002).
4. Z. X. Bian, B. Liu, and A. Shakouri, "InP-based passive ring-resonator-coupled lasers," *IEEE Photonics Technol. Lett.* **39**(7), 859–861 (2003).
5. J. M. Choi, R. K. Lee, and A. Yariv, "Control of critical coupling in a ring resonator fiber configuration: application to wavelength selective switching, modulation, amplification and oscillation," *Opt. Lett.* **26**(16), 1236–1238 (2001).
6. C. K. Madsen, G. Lents, A. J. Bruce, M. A. Capuzzo, L. T. Gomez, T. N. Nielsen, and J. Brener, "Multistage dispersion compensator using ring resonators," *Opt. Lett.* **24**(22), 1555–1557 (1999).
7. B. E. Little and S. T. Chu, "Microring resonators for very large scale integrated photonics," *Proc. SPIE* **3890**, 487–488 (1999).
8. S. T. Chu, B. E. Little, W. Pan, T. Kaneko, S. Sato, and Y. Kokubun, "An eight-channel add-drop filter using vertically coupled microring resonators over a cross grid," *IEEE Photonics Technol. Lett.* **11**(6), 691–693 (1999).
9. S. Suzuki, Y. Hatakeyama, Y. Kokubun, and S. T. Chu, "Precise control of wavelength channel spacing of microring resonator add–drop filter array," *J. Lightwave Technol.* **20**(4), 745–750 (2002).
10. A. Vörckel, M. Mönster, W. Henschel, P. H. Bolivar, and H. Kurz, "Asymmetrically coupled silicon-on-insulator microring resonators for compact add–drop multiplexers," *IEEE Photonics Technol. Lett.* **15**(7), 921–923 (2003).
11. C. K. Madsen and J. H. Zhao, *Optical Filter Design and Analysis: A Signal Processing Approach*, Wiley, New York (1999).
12. E. A. J. Marcatili, "Dielectric rectangular waveguide and directional coupler for integrated optics," *Bell Syst. Tech. J.* **48**(7), 2071–2102 (1969).
13. E. A. J. Marcatili, "Bends in optical dielectric guides," *Bell Syst. Tech. J.* **48**(7), 2103–2132 (1969).
14. A. Yariv, *Optical Electronics in Modern Communications*, 5th ed., Chap. 13, pp. 491–540, Oxford University Press, London (1997).
15. K. Oda, N. Takato, and H. Toba, "A wide-FSR waveguide double-ring

resonator for optical FDM transmission system,'' *J. Lightwave Technol.* **9**(6), 728–736 (1991).
16. C. Manolatou, M. J. Khan, S. Fan, P. R. Villeneuve, H. A. Haus, and J. D. Joannopoulos, ''Coupling of modes analysis of resonant channel add drop filters,'' *IEEE J. Quantum Electron.* **35**(9), 1322–1331 (1999).

Chun-Sheng Ma received his BSc and MSc degrees in optoelectronics from Jilin University, Changchun, China, in 1969 and 1982, respectively, where he is currently a professor in the College of Electronic Science and Engineering and the State Key Laboratory on Integrated Optoelectronics. His main areas of research are guided-wave optics, nonlinear optics, and integrated optoelectronics, and his interests include the characteristic analysis and computer-aided design of optoelectronic devices. His more than 80 papers have been published in international and Chinese journals. His research results were evaluated as the National Science and Technology Achievements by the Chinese Science and Technology Council in 1988 and 1991, respectively. He was awarded the Science and Technology Progress Awards of the Chinese Educational Council in 1990 and 1998, respectively.

Xian-Yin Wang received his BSc degree in physics and MSc degree in atomic and molecular physics from Shandong Normal University, Jinan, China, in 1995 and 1998, respectively, and received his PhD degree in theoretical physics from Jilin University, Changchun, China in 2004. Currently he is pursuing postdoctoral study at Changchun University of Science and Technology, Changchun, China. His main areas of research are guided-wave optics and integrated optoelectronics, and his interests include the characteristic analysis and computer-aided design of optoelectronic devices.

Biographies and photographs of other authors not available.